ATP/GTP Hydrolysis Is Required for Oxazole and Thiazole Biosynthesis in the Peptide Antibiotic Microcin B17†

Jill C. Milne, Andrew C. Eliot, Neil L. Kelleher, and Christopher T. Walsh*

Department of Biological Chemistry and Molecular Pharmacology Harvard Medical School, Boston, Massachusetts 02115

Received May 1, 1998

ABSTRACT: In the maturation of the *Escherichia coli* antibiotic Microcin B17, the product of the *mcbA* gene is modified posttranslationally by the multimeric Microcin synthetase complex (composed of McbB, C, and D) to cyclize four Cys and four Ser residues to four thiazoles and four oxazoles, respectively. The purified synthetase shows an absolute requirement for ATP or GTP in peptide substrate heterocyclization, with GTP one-third as effective as ATP in initial rate studies. The ATPase/GTPase activity of the synthetase complex is conditional in that ADP or GDP formation requires the presence of substrate; noncyclizable versions of McbA bind to synthetase, but do not induce the NTPase activity. The stoichiometry of ATP hydrolysis and heterocycle formation is 5:1 for a substrate that contains two potential sites of modification. However, at high substrate concentrations ($>50K_m$) heterocycle formation is inhibited, while ATPase activity occurs undiminished, consistent with uncoupling of NTP hydrolysis and heterocycle formation at high substrate concentrations. Sequence homology reveals that the McbD subunit has motifs reminiscent of the Walker B box in ATP utilizing enzymes and of motifs found in small G protein GTPases. Mutagenesis of three aspartates to alanine in these motifs (D132, D147, and D199) reduced Microcin B17 production in vivo and heterocycle formation in vitro, suggesting that the 45 kDa McbD has a regulated ATPase/GTPase domain in its N-terminal region necessary for peptide heterocyclization.

Peptides with antibiotic activity often undergo substantial posttranslational modification to produce stable molecules with bioactivity. For example, the dehydration of serine residues and subsequent cross-linking to cysteine residues produces the lanthionine moieties found in the lantibiotic peptides (*1*), and the oxygenative cyclization of *δ*-(L-α-aminoadipoyl)-L-cysteinyl-D-valine (ACV) by isopenicillin N synthase yields the bicyclic *β*-lactam antibiotic skeleton (*2*). There is a large class of peptide natural products that contain one or more of the five-membered ring heterocycles, oxazoles and thiazoles. These structures are of interest both because of their interactions with diverse intracellular targets and mechanism of heterocycle biosynthesis.

Oxazoles in peptides arise by cyclization of the side chain of serine residues on the immediate upstream peptide carbonyl linkage, followed by water elimination to the oxazoline and dehydrogenation to the heteroaromatic ring; similarly the intramolecular attack of the cysteine thiolate side chain on the preceding peptide bond initiates the cyclization-dehydration-dehydrogenation sequence to yield thiazole. As noted in Scheme 1, Gly-Ser dipeptide moieties would yield the aminomethyloxazole moiety, while Gly-Cys dipeptide moieties would yield the corresponding thiazole heterocycle.

The widely prescribed anticancer drug bleomycin uses an aminoethyl bithiazole moiety (presumably from an Asp-Cys-Cys precursor) to intercalate into DNA and the subsequent oxygenative double-strand breaks that occur are the basis for its therapeutic activity (*3*). The polythiazole peptide antibiotics thiostrepton (*4*) and GE2270A (*5*) act by inhibiting translation steps in bacterial protein synthesis, while the thiazoline-containing dodecapeptide bacitracin (*6*) blocks bacterial cell wall biosynthesis by complexation with bactoprenol-PP. Strains of *Escherichia coli* also produce a peptide antibiotic, Microcin B17 (MccB17),[1] containing thiazole and oxazole rings (*7*−*9*). Biosynthesis and secretion of MccB17 requires the activities encoded by seven open reading frames, *mcbABCDEFG* (Figure 1A) (*10, 11*). The mature antibiotic contains four thiazole and four oxazole rings and is reported to kill sensitive strains of *E. coli* by inhibiting DNA gyrase (*12*). *mcbA* encodes the 69 amino acid prepro-antibiotic. Genetic studies have shown McbB, C, and D are required for maturation to the thiazole- and oxazole-containing proMccB17 (Figure 1B) (*13, 14*), and we have recently reported the purification of a MccB17 synthetase complex containing the three subunits McbB, C, and

Scheme 1

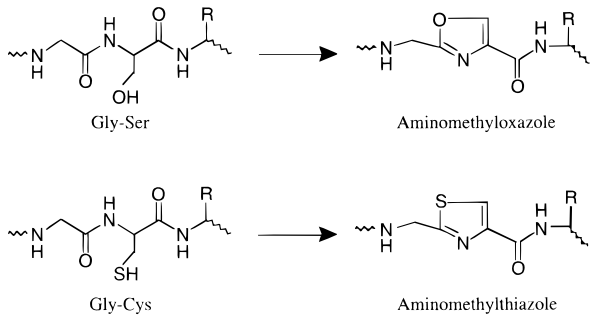

†This research was supported by NIH Grant GM 20011 to C.T.W. J.C.M. is an American Cancer Society Postdoctoral Research Fellow (Grant PF4332). N.L.K. is an NIH Postdoctoral Research Fellow and also received support from the Armenise Foundation.

* To whom correspondence should be addressed. Phone: 617-432-1715. Fax: 617-432-0556. E-mail: walsh@walsh.med.harvard.edu.

S0006-2960(98)00996-9 CCC: $15.00
Published on Web 08/28/1998

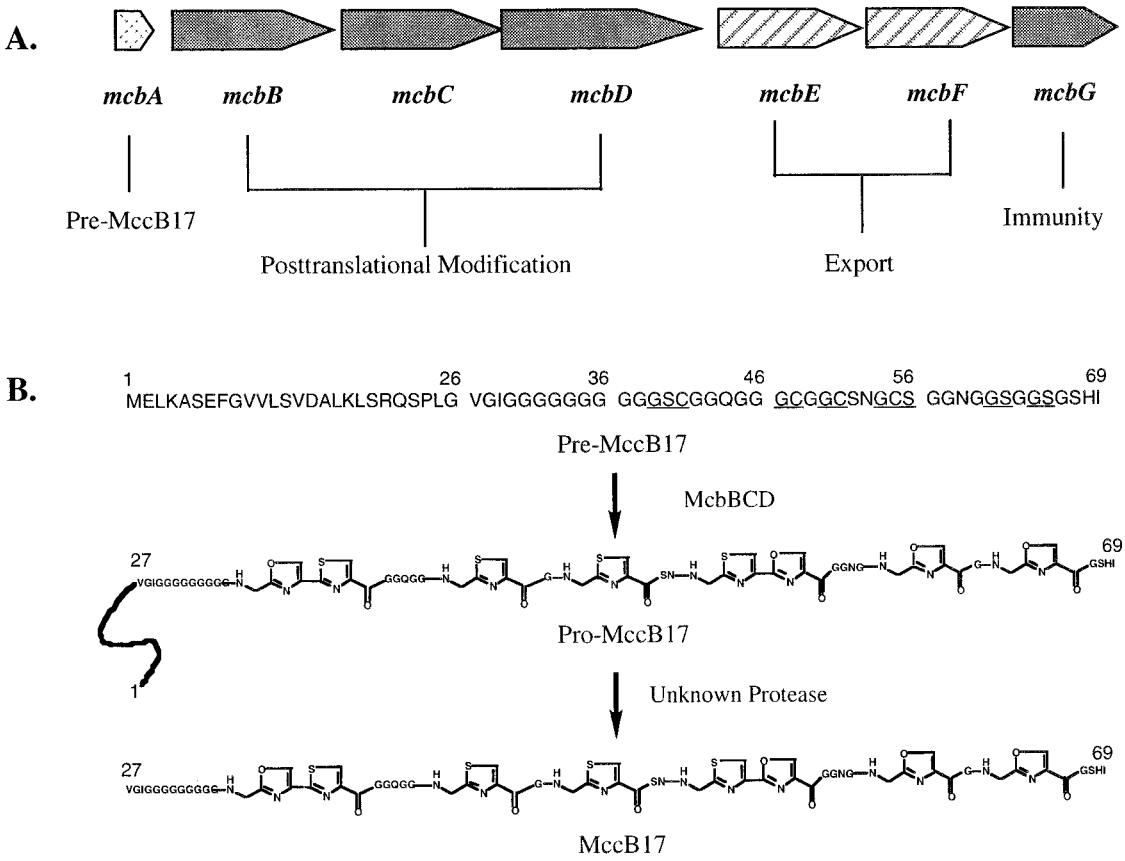

FIGURE 1: (A) MccB17 operon. (B) Maturation of MccB17. The 69 amino acid pre-MccB17 is processed by MccB17 synthetase to create pro-MccB17 incorporating eight heterocycles—four oxazoles and four thiazoles. Serines and cysteines that are cyclized are underlined. The N-terminal 26 amino acid propeptide is removed by an unknown *E. coli* protease to release the mature antibiotic, MccB17.

D that is active in heterocycle formation (*14*). The amino-terminal 26 amino acids are removed by an as yet unidentified *E. coli* protease, and the mature MccB17 is secreted by the action of McbE and F that are thought to form an ABC type transporter (*15*). McbG is an immunity protein of undefined mechanism that protects the producing cell from the cytotoxic activity of MccB17 (*15*).

MccB17 synthetase is the first peptide thiazole and peptide oxazole synthesizing enzyme complex to be isolated and offers prospects for insights into specificity and mechanism of heterocyclizations which alter peptide backbone connectivity, nitrogen basicity, and in the case of tandem cyclizations of adjacent residues, create DNA intercalators. To date we have delineated issues of selectivity at the first site in the McbA substrate, $Gly_{39}Ser_{40}Cys_{41}$, that yields the 4,2-fused oxazole-thiazole in wild-type McbA (*16*). We have noted an absolute requirement for the propeptide, residues 1−26, to be fused in cis, upstream of a heterocyclizable di- or tripeptide moiety (*14, 17, 18*). This observation means that all substrates must encompass at least the first 40 residues of McbA. We have utilized both full-length His_6-McbA fusion proteins (*14*), full-length fusions of McbA to either β-galactosidase or maltose-binding protein (MBP-McbA) (*14, 17*), and MBP fusions to the first 46 residues of McbA (MBP-$McbA_{1-46}$) (*16*) as substrate analogues in synthetase assays. The latter is the preferred substrate in the studies reported here.

In addition to the specificity conferred by the propeptide, a second unanticipated feature of MccB17 synthetase catalyzed heterocyclization was our preliminary demonstration of a requirement for ATP to produce oxazole or thiazole-containing heterocyclic products (*14*). Experiments to evaluate the role of ATP in Ser and Cys conversion to oxazole and thiazole and a candidate subunit for the ATPase are the subject of this work.

EXPERIMENTAL PROCEDURES

Materials. Bacteriological media were obtained from Difco Laboratories. Competent *E. coli* strain BL21DE3 [F^-, *ompT*, *hsdS*$_B$, (r_B^-, m_B^-), *gal*, *dcm*, (DE3)] was obtained from Novagen. Competent *E. coli* strain DH5α [F^-, f80d*lacZ*ΔM15, Δ(*lac*ZYA-*arg*F)U169, *deo*R, *rec*A1, *end*A1 *hsd*R17(r_K^-, m_K^+), *pho*A, *sup*E44, l^-, *thi*-1, *gyr*A96, *rel*A1] and plasmid pUC19 were purchased from Gibco BRL. Restriction endonucleases, T4 DNA ligase, dNTPs, and amylose resin were obtained from New England Biolabs. Calmodulin affinity resin and *Pfu* DNA polymerase were

[1] ABBREVIATIONS: AMP-CPP, α,β-methyleneadenosine 5′-triphosphate; AMP-PCP, β,γ-methyleneadenosine 5′-triphosphate; ATPγS, adenosine 5′-*O*-(3-thiotriphosphate); CBP, calmodulin-binding peptide; dNTP, deoxynucleotide triphosphate; DTT, dithiothreitol; EDTA, ethylenediaminietetraacetic acid (disodium salt); EGTA, ethylene glycol bis(β-aminoethyl ether)-*N*,*N*,*N*′,*N*′-tetraacetic acid; ESI-MS, electrospray ionization mass spectrometry; HPLC, high-performance liquid chromatography; IPTG, isopropyl 1-thio-β-D-galactosidase; LB, Luria−Bertani medium; MBP, maltose-binding protein; MccB17, Microcin B17; MS, mass spectrometry; PAGE, polyacrylamide gel electrophoresis; PCR, polymerase chain reaction; PMSF, phenylmethanesulfonyl fluoride; SOE, splicing by overlap extension; TLC, thin-layer chromatography; UV, ultraviolet; WT, wild-type.

obtained from Stratagene. Isopropyl 1-thio-β-D-galactopyranoside (IPTG) was purchased from Bachem Biosciences. Kanamycin and ampicillin were obtained from Sigma. [^{32}P]α-ATP (10 mCi/mL; 3000 Ci/mmol) and [^{32}P]α-GTP (10 mCi/mL; 3000 Ci/mmol) were obtained from New England Nuclear. ATP, GTP, adenosine 5′-*O*-(3-thiotriphosphate) (ATPγS), ITP, XTP, β,γ-methyleneadenosine 5′-triphosphate (AMP-PCP), α,β-methyleneadenosine 5′-triphosphate (AMP-CPP), UTP, and CTP were obtained from Sigma and were of the highest grade available. Low molecular weight markers were obtained from Bio-Rad. The synthetic peptides McbA$_{1-46(\Delta 30-37)}$ and McbA$_{1-26}$−CONH$_2$ (*18*) were synthesized at the Howard Hughes Biopolymer Facility at Harvard Medical School using solid-phase Fmoc-based peptide synthesis on an automated peptide synthesizer (*19*). Plasmids, pMSS36, and pMSS37 encoding the MBP-McbA$_{1-46(GSG)}$ and MBP-McbA$_{1-46(GGC)}$ fusion proteins will be described elsewhere (*20*).

Recombinant DNA Methods. Recombinant DNA techniques were performed as described elsewhere (*21*). Preparation of plasmid DNA, gel purification of DNA fragments, and purification of polymerase chain reaction (PCR) amplified products were performed using a QIAprep spin plasmid kit, a QIAEX II gel extraction kit, and a QIAquick PCR purification kit, respectively (Qiagen). Oligonucleotide primers were obtained from Integrated DNA Technologies or Gene Link. PCR reactions were performed in 100 μL containing 1× *Pfu* polymerase reaction buffer (Stratagene), 200 μM each dNTP, 1 μM each PCR primer, approximately 200 ng of plasmid template, and 2.5 units of cloned *Pfu* polymerase. The fidelity of PCR products was confirmed by nucleotide sequencing after subcloning into the appropriate expression vector. DNA sequencing was performed by the Molecular Biology Core Facility of the Dana Farber Cancer Institute (Boston, MA).

Overexpression and Purification of CBP-Tagged MccB17 Synthetase. The MccB17 synthetase expression vector pCALBCDn overexpresses calmodulin binding peptide-McbB (CBP-McbB), McbC, and McbD under the control of the T7 promoter and allows a one step purification of CBP-tagged MccB17 synthetase on calmodulin affinity resin (*16*). Overexpression and purification of CBP-tagged MccB17 synthetase was performed with some modifications to the previously described method (*16*).

Briefly, overnight cultures of LB medium supplemented with ampicillin (100 μg/mL) were inoculated from a frozen stock of pCALBCDn/BL21DE3 and grown at 37 °C. Aliquots (6 × 10 mL) were used to inoculate 6 × 1 L of LB-ampicillin. Cultures were grown at 37 °C to an OD$_{600}$ of 0.6−0.8 and induced with 400 μM IPTG. Cells were harvested 3 h later by centrifugation. Cell pellets were resuspended in buffer A (50 mM Tris pH 7.5, 150 mM NaCl, 1 mM DTT, and 2 mM $CaCl_2$) and frozen at −80 °C. The cells were thawed and protease inhibitors were added (2 μg/mL aprotinin, 1 μg/mL chymostatin, 1 μg/mL leupeptin, and 100 μM PMSF). The cells were disrupted twice in a French pressure cell (18 000 PSI) and cellular debris was removed by centrifugation (18000*g*, 30 min). The supernatant was applied to a calmodulin column (1.5 mL bed volume) previously equilibrated with buffer A. The column was washed with buffer A (50 mL) and then with 50 mL of buffer B (50 mM Tris pH 7.5, 150 mM NaCl, 1 mM DTT, and 2 mM EGTA). During the latter wash, CBP-tagged MccB17 synthetase begins to elute from the column but these fractions contain significant contaminating ATPases. Higher purity MccB17 synthetase was then eluted with buffer C (50 mM Tris pH 7.5, 300 mM NaCl, 1 mM DTT, and 0.1% Triton X-100). Fractions containing CBP-MccB17 synthetase were analyzed for purity by SDS−PAGE, pooled, aliquoted, and stored at −80 °C. Protein concentration was determined using the Coomassie Plus Protein Assay Reagent (Pierce) with BSA as a standard.

Construction of MBP-McbA. The expression vector for the maltose-binding protein-McbA fusion protein (MBP-McbA), pETMBP-McbA, was constructed from plasmid pLARA15b (*14*), which is a pET15b derivative that encodes hexahistidine-tagged McbA. Briefly, the sequence coding for the hexahistidine tag (*Nco*I−*Nde*I) was replaced by the *Nco*I−*Nde*I fragment from plasmid pIADL14, that encodes the maltose-binding protein followed by a thrombin cleavage site (LVPRGS) (*22*). For expression of MBP-McbA, plasmid pETMBP-McbA was transformed into *E. coli* strain BL21DE3.

Overexpression and Purification of MccB17 Synthetase Substrates. The MBP-fusion substrates, MBP-McbA, MBP-McbA$_{1-46}$, MBP-McbA$_{1-46(GSG)}$, and MBP-McbA$_{1-46(GGC)}$ were maintained as frozen stocks in *E. coli* strain, BL21DE3. For expression, 10 mL of an overnight culture was used to inoculate 1 L of LB-ampicillin (100 μg/mL). Cultures were grown at 37 °C and induced with 1 mM IPTG at an OD$_{600}$ of 0.6−0.8. After 3 h of induction, the cells were harvested by centrifugation and resuspended in 20 mL of buffer A1 (20 mM Tris, pH 7.5, and 200 mM NaCl). The cells were disrupted twice in a French pressure cell (18 000 PSI) and cellular debris was removed by centrifugation (18000*g*, 30 min). The supernatant was applied to an amylose column (15−20 mL bed volume). The column was washed with 20 column volumes of buffer A1, and the MBP fusion protein was eluted with buffer B1 (20 mM Tris, pH 7.5, 200 mM NaCl, and 10 mM maltose). Fractions (5 mL each) containing the protein were combined, concentrated in a Centriprep 30 concentration unit (Millipore), aliquoted, and stored at −80 °C. Protein concentration was determined by UV−vis spectroscopy (ϵ_{280} = 66 350 M^{-1} cm^{-1} for all fusion proteins) (*23*).

Western Blot Assay for Synthetase Activity. Reaction mixtures consisted of 20 μM MBP-McbA$_{1-46}$ fusion protein (unless otherwise noted), 1× MccB17 synthetase buffer (50 mM Tris pH 7.5, 100 mM NaCl, 20 mM $MgCl_2$, 10 mM DTT, and 2 mM ATP) and CBP-tagged MccB17 synthetase (0.05 mg/mL). Reactions were incubated at 37 °C, aliquots were removed at the times indicated in the figure legends, quenched with SDS−PAGE sample buffer, and electrophoresed on a 10% SDS−PAGE gel. The gels were transblotted to Immobilon-P PVDF membranes (Millipore) at 60 V for 60 min and analyzed by protein immunoblotting with rabbit polyclonal anti-MccB17 antibodies (*13*) and goat anti-rabbit Horseradish Peroxidase conjugated antibodies [IgG (H+L); Pierce]. The signal was detected on film (Reflection, Dupont New England Nuclear) using the chemiluminescent SuperSignal detection system (Pierce). The chemilumenescent substrate was diluted 1:5 with water and incubated with the immunoblot for 3 min to avoid signal

Table 1: Oligonucleotide Primers for Site-Directed Mutagenesis

primer	code	5′−3′ nucleotide sequence
EagI	1	GAGCGTATTACACCAGCCAGCGCGGC
SalI	2	GAACGAATAAATAATAGTCGACCATCC
K49A	3	CGTATTACACCAGCCAGCGCGGCCGGTGAAACTCTGGCGTC
G45A	4	CCAGCCAGCGCGGCCGCTGAAACTCTGAAGTCAATTCAGGG
D132A	5	GCAGTCATAATTGCACTCGCCAATATAACCGCTGC
D132A	6	GCAGCGGTTATATTGGCGAGTGCAATTATGACTGC
D147A	7	CTGAAATTTTATCCTGACAGAGCTACATGCGGATGTAG
D147A	8	CTACATCCGCATGTAGCTCTGTCAGGATAAAATTTCAG
G150A	9	GACAGAGATACATGCGCATGTAGCTTTCATGG
G150A	10	CCATGAAAGCTACATGCGCATGTATCTCTGTC
N196A	11	GAAATAGTAACAGGCATAGCTCATATAGATGAG
N196A	12	CTCATCTATATGAGCTATGCCTGTTACTATTTC
D199A	13	GGCATAAATCATATAGCTGAGATTTTACTGGC
D199A	14	GCCAGTAAAATCTCAGCTATATGATTTATGCC

saturation. Developed films were scanned and quantified using the NIH image software package (Version 1.61; NIH).

ATPase/GTPase Assays. Reaction mixtures consisted of 1× MccB17 synthetase buffer, 0.01 μCi/mL [^{32}P]α-ATP, 20 μM MBP-McbA$_{1-46}$ (unless otherwise noted), and CBP-MccB17 synthetase (0.05 mg/mL) in a total volume of 60 μL. Assays were performed at 37 °C. Aliquots (5 μL) were removed at t = 0, 10, 20, 30, 40, 50, and 60 min, and quenched with 15 μL 0.5 M EDTA. Samples (1 μL) were spotted onto polyethyleneimine cellulose plates with a fluorescence indicator (Polygram CEL300/UV 254; Aldrich Chemical Co., Inc.) and developed by chromatography in 0.75 M postassium phosphate (pH 3.5). Solutions (10 mg/mL) of unlabeled ATP, ADP, and AMP were co-chromatographed and visualized by UV as references. The plates were dried and the radioactivity was visualized by exposure to a Fuji imaging plate and quantified on a Fuji Imager using the Image Gauge Software package (Version 3.0).

GTPase activity was measured using the assay as described except that 2 mM GTP and 0.01 μCi/mL [^{32}P]α-GTP were substituted for the ATP stocks. As controls for contaminating ATPases/GTPases, reactions were run with MccB17 synthetase alone and for each substrate alone. ATPase/GTPase activity associated with the substrate alone was negligible, while that for the enzyme alone was detectable. Unless otherwise noted, the ATPase/GTPase activities reported for reactions containing MccB17 synthetase and substrate were corrected using the activity obtained for enzyme alone under the same conditions but not for substrate alone.

HPLC and Mass Spectrometric Analysis. Reaction mixtures consisted of 20 μM MBP-McbA$_{1-46}$ fusion protein, 50 mM Tris pH 7.5, 100 mM NaCl, 20 mM $MgCl_2$, 10 mM DTT, 2 mM ATP, and CBP-tagged MccB17 synthetase (0.05 mg/mL). Reactions were incubated at 37 °C, aliquots were removed at t = 0, 15, 30, 45, and 60 min and quenched with 1 M urea-0.2 M Tris, pH 7.5. The MBP tag was removed by digestion with thrombin (0.025 unit/mL; 3 h at 25 °C).

The cleaved McbA$_{1-46}$ fragments were purified on an analytical C18 reversed-phase HPLC column (Vydac) using a Beckman System Gold HPLC. Solvent A was water-0.1% TFA and solvent B was acetonitrile-0.1% TFA. A linear gradient (30 to 42% solvent B) was run over 12 min. Peaks were detected on line with a Beckman 168 diode array spectrophotometer. The M, M-20, and M-40 species co-eluted at 7.8 min. Peaks were collected and samples were dried under vacuum.

For electrospray ionization (ESI) (*24*), samples were dissolved in 10−25 μL of 50:49:1 H_2O:CH_3CN:CH_3COOH and 1−10 μL was injected into a 0.5 m fused silica capillary. The sample plug was infused at 2 μL/min into the pneumatically assisted ESI source of a Micromass Quatro II triple-quadrupole MS (Beverly, MA), maintained at the Boston University NIH MS Resource Center. Spectra were acquired over the 500−2500 *m*/*z* range at 10 s/scan and deconvoluted using MaxEnt software. Ratios of M, M-20, and M-40 were determined by peak heights and no abundance corrections for cationic adducts (e.g., sodium = +22 Da) were made, as these were typically less than 15% relative abundance. Also, the ionization efficiencies for the M, M-20, and M-40 components were assumed to be similar, an assumption validated in a separate study (*20*). Average mass values are reported and mass accuracy is 0.01−0.02%.

Construction of pUC19-mccb17. The entire MccB17 biosynthetic operon (*mcbABCDEFG*) was cloned into the high copy expression vector, pUC19, to create the MccB17 production plasmid, pUC19mccb17. Briefly, a *Bam*HI−*Bst*BI fragment encoding *mcbABCDEF* and part of *mcbG*, from plamid pPY113 [a pBR322 plasmid containing the MccB17 operon (*13*)] was gel purified. The remaining sequence of *mcbG* was amplified by PCR introducing a *Sph*I site at the 3′-terminus. The PCR product was digested with *Bst*BI and *Sph*I and gel purified. A ligation was performed with the fragments pPY113 (*Bam*HI−*Bst*BI), *mcbG* PCR product (*Bst*BI−*Sph*I), and pUC19 (*Bam*HI−*Sph*I). The ligation was transformed into *E. coli* strain DH5α and the desired clone was identified by restriction mapping.

Site-Directed Mutagenesis of mcbD. Site-directed mutants in *mcbD* (D132A, D147A, G150A, N196A, and D199A) were constructed in pUC19mccb17 using the splicing by overlap extension method (SOE). The sense/antisense primer pairs are shown in Table 1. In the first round of PCR, the sequence upstream and downstream of the mutation was amplified in separate reactions using pUC19mccb17 as template. The primer pairs for the mutants D132A, D147A, G150A, N196A, and D199A were 1/6 and 2/5; 1/8 and 2/7; 1/10 and 2/9; 1/12 and 2/11; and 1/14 and 2/13; respectively. The PCR products were gel purified and used as templates in the second round of PCR using the *Eag*I and *Sal*I primers. The PCR product was purified, digested with *Eag*I and *Sal*I, gel purified, and subcloned into the *Eag*I and *Sal*I digested

pUC19mccb17. The site-directed mutants G45A and K49A were constructed by PCR using a mutagenic 5′ PCR primer (G45A primer 4 and K49A primer 3) and the *Sal*I primer. The PCR products were gel purified, digested with *Eag*I and *Sal*I, gel purified, and subcloned into the *Eag*I and *Sal*I digested pUC19mccb17.

Site-directed mutants in *mcbD* (G45A, K49A, D132A, D147A, and D199A) were constructed in pCALBCDn by subcloning the *Ava*I−*Sal*I fragments from the pUC19mccb17 mutant constructs described above. Briefly, the two fragments, *Bam*HI−*Ava*I and *Bam*HI−*Sal*I were purified from pCALBCDn and an *Ava*I−*Sal*I fragment from each McbD mutant was purified from digested pUC19mccb17 mutant plasmids. The three fragments, *Bam*HI−*Ava*I from pCALBCDn, *Bam*HI−*Sal*I from pCALBCDn, and *Ava*I−*Sal*I from the mutant pUC19mccb17 plasmids, were ligated and transformed into DH5α. The presence of the appropriate mutation was confirmed by DNA sequencing, and the plasmids were transformed into BL21DE3 for overexpression of the mutant CBP-tagged MccB17 synthetases.

Preparation of Crude Cell Extracts of Mutant and Wild-Type pUC19mccb17/DH5α Strains. Frozen stocks of pUC19mccb17/DH5α wild-type and mutant strains were used to inoculate 4 mL cultures of LB-ampicillin (100 μg/mL). After 18−24 h of growth at 37 °C, 2 mL of each culture was used to inoculate 100 mL of M63-glucose media (100 μg/mL ampicillin). The cultures were grown at 37 °C for 18−24 h. The cells were collected by centrifugation, resuspended in 2 mL of 50 mM Tris, pH 7.5, and 100 mM NaCl, and lysed using a Branson microtip sonicator probe (30 s total; 10−50% duty cycle over 5 s; output control 6, pulse setting). The lysates were cleared of cellular debris by centrifugation and the supernatant was aliquoted and stored at −80 °C. Protein concentrations were determined using the Coomassie Plus Protein Assay Reagent (Pierce) with BSA as a standard.

Bioassay for MccB17 Antibiotic Activity. Frozen stocks of pUC19mccb17/DH5α wild-type and mutant strains were used to inoculate 2 mL cultures of LB-ampicillin (100 μg/mL). After 18−24 h of growth at 37 °C, the cells were collected by centrifugation, and resuspended in 20 mL of M63-glucose media (100 μg/mL ampicillin), and grown at 37 °C for 18−24 h. The OD_{600} was determined, and the cells were pelleted and resuspended in lysis buffer (100 mM acetic acid-1 mM EDTA) at 1 OD unit/mL. The extracts were boiled for 10 min, and cellular debris was removed by centrifugation. The supernatant contained the MccB17 antibiotic and was aliquoted and stored at −80 °C.

For the liquid culture bioassay, an overnight culture of a MccB17-sensitive *E. coli* strain, ZK4, was diluted 1:100 into 2 mL of fresh LB. Antibiotic-containing extracts prepared as described above from the mutant or wild-type strains were added (0, 5, 10, 20, 40, 60, and 80 μL). After the cultures were grown at 37 °C for 5 h, the OD_{600} was determined.

RESULTS

ATP or GTP Is Required for Oxazole and Thiazole Formation. In every experiment with purified MccB17 synthetase and with every analogue of McbA substrate, there was an absolute requirement for ATP in order to detect heterocyclization activity. In the experiments presented in this paper, a calmodulin-binding peptide-tagged version of MccB17 synthetase was used, because it allowed a one step affinity purification of the three subunit enzyme (*16*). Equivalent data are seen with enzyme complex isolated by nonaffinity strategies.

The data of Figure 2 are representative and show a time course over 90 min of incubation of substrate MBP-McbA with purified MccB17 synthetase. The assay is a Western assay using a polyclonal antibody (*13*) that specifically recognizes thiazoles and oxazoles (*14*, *20*). The data from the Western assay in Figure 2A are plotted in Figure 2B to show that the assay gives a linear response for initial velocity studies. No heterocyclic product is detectable when ATP is omitted. GTP can substitute as shown by the middle panel in Figure 2A, but with a diminished rate of heterocycle formation. The purine ITP was also a substrate, while XTP was not (data not shown). No activity was seen with the pyrimidine triphosphates, UTP or CTP (data not shown).

The kinetic parameters for the various purine triphosphate analogues are shown in Table 2. The K_m for ATP was 92 μM, while GTP and ITP had K_m values of 38 and 354 μM, respectively. At V_{max}, ATP had a 3-fold higher rate than GTP, such that V_{max}/K_m catalytic efficiency ratios are comparable. ITP had an approximately 3-fold lower rate than ATP. ATPγS was processed with a K_m of 141 μM, but a 76-fold drop in V_{max}, as might be anticipated if $-PO_3$ transfer is partly rate limiting given the decrease in reactivity of the PSO_2 group in attack by nucleophiles. When the side-chain methylene analogues of ATP were tested, the AMP-CPP analogue was neither a substrate nor an inhibitor, while the AMP-PCP was an effective competitive inhibitor (K_i = 2.3 μM; data not shown) but had no substrate activity. Thus, cleavage of ATP or GTP is required for heterocycle formation. When [^{32}P]α-ATP was utilized, the product was radioactive ADP, as shown in Figure 2C.

Substrate Dependence of the ATPase/GTPase Activity of Microcin Synthetase. When MccB17 synthetase was incubated with either MBP-$McbA_{1-46}$ or MBP-McbA, a rate of ATP hydrolysis of 1.6 μM ATP/min was observed for both substrates under initial velocity conditions (Figure 3). While the MBP-$McbA_{1-46}$ contains only the first two heterocyclization sites, the MBP-McbA contains all eight sites. The ability of these two substrates to induce the same rate of ATPase activity in MccB17 synthetase may be due to the fact that they exhibit the same initial rates of heterocyclization for first and possibly second ring formation.

In prior studies, we have shown that the propeptide $McbA_{1-26}$ (residues 1−26 of McbA) has a K_i of 2 μM, equivalent to the K_m of full-length McbA (K_m = 2 μM), while the synthetic peptide $McbA_{27-46}$ (residues 27−46 of McbA) was not detectably bound or processed, indicating that initial recognition was provided by binding to the propeptide region and not the cyclizable site at $G_{39}S_{40}C_{41}$ (*14*). When synthetic $McbA_{1-26}-CONH_2$ was incubated with pure synthetase, it did not induce the ATPase activity of the synthetase even though it has high affinity (Figure 3). Figure 3 also shows that a synthetic peptide [$McbA_{1-46(\Delta 30-37)}$] with an eight glycine stretch, $G_{30}-G_{37}$, deleted does not induce ATPase activity. In separate studies, we have shown that this deletion mutant, even though it has the GSC tripeptide moiety downstream of the propeptide, is

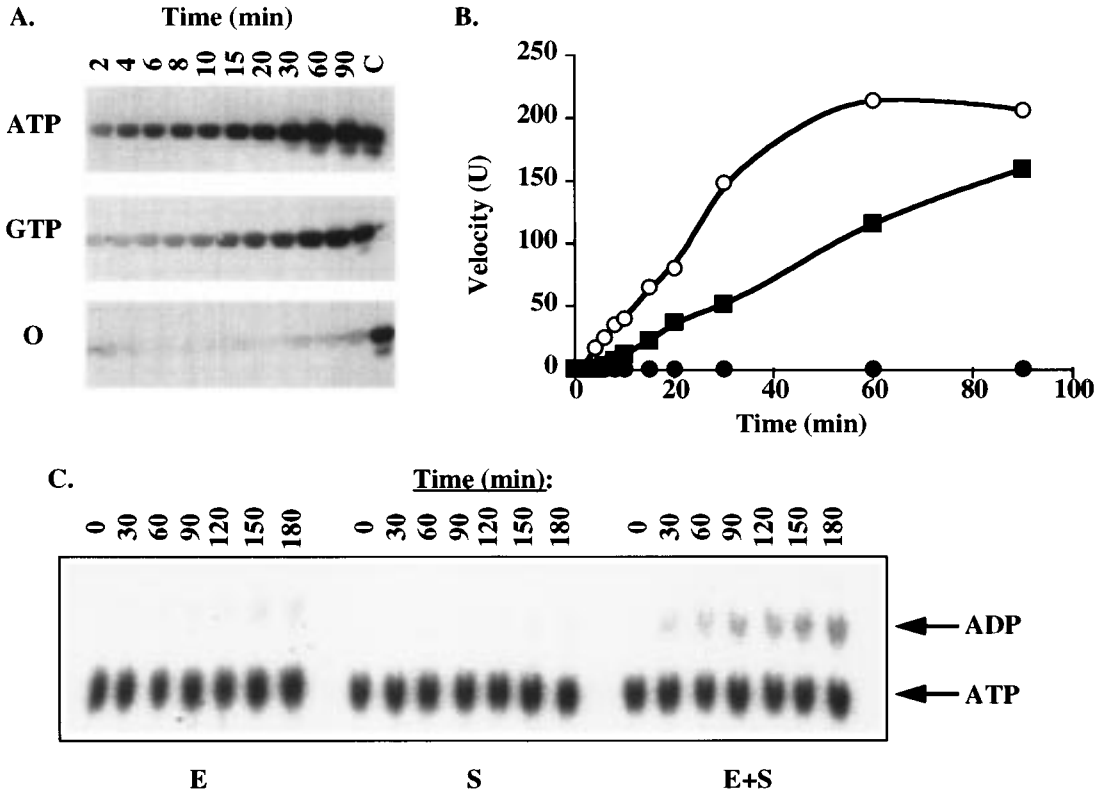

FIGURE 2: ATP or GTP is required for heterocycle formation. (A) Western blot analysis of MccB17 synthetase reactions performed in the presence of ATP, GTP, or no nucleoside triphosphate using 20 μM MBP-McbA$_{1-46}$ as substrate. Reactions were performed at 37 °C as described in the Experimental Procedures. At t = 0, 2, 4, 6, 8, 10, 15, 20, 30, 60, and 90 min, an aliquot was removed from each reaction and quenched. Samples were run on SDS−PAGE followed by Western blotting as described in the Experimental Procedures. A positive control used for normalization of Western blots was run in lane C. (B) Plot of Western data from panel A. Data are normalized against the control lane run on each gel. ATP (○), GTP (■), and 0 (●). (C) ATPase assay. Incubations containing 1× MccB17 synthetase assay buffer, [^{32}P]α-ATP, and either MccB17 synthetase alone, 20 μM MBP-McbA$_{1-46}$ substrate alone, or MccB17 synthetase plus 20 μM MBP-McbA$_{1-46}$ were performed at 37 °C. At the time points indicated, aliquots were removed, quenched, and analyzed by TLC followed by audoradiography.

Table 2: Kinetic Parameters for MccB17 Synthetase

substrate	K_m[a] (μM)	rate[b] (OD units/min)	relative rate[c]	relative[d] k_{cat}/K_m
ATP	92	6.7	1	1
GTP	38	2.2	0.33	1/1.26
ATPγS	141	0.088	0.013	1/117
ITP	354	2.8	0.35	1/10

[a] The K_m for ATP and GTP were determined using the ATPase assay, while the K_m's for ATPγS and ITP were determined using a Western blot assay. [b] All rates were determined using a Western blot assay.[c] The rates are expressed relative to the rate with ATP as substrate. [d] The catalytic efficiency (k_{cat}/K_m) for each substrate is expressed relative to the k_{cat}/K_m determined for ATP.

out of register and, though it binds well to synthetase, is not detectably heterocyclized [Y.M.Li, A.C.E., and C.T.W., unpublished experiments (*16*)]. The data obtained with the synthetic peptides strongly suggest coupling of the conditional ATPase/GTPase activity to actual substrate processing.

Stoichiometry of ATP Hydrolysis and Heterocycle Formation. To assess the stoichiometry of ATP cleavage to ring formation, we carried out a time course for processing of 20 μM MBP-McbA$_{1-46}$ by 530 nM MccB17 synthetase. Under these conditions, [^{32}P]α-ADP production was followed over the course of 1 h by a TLC assay. In a parallel reaction following heterocycle formation, aliquots were removed at time points of 0, 15, 30, 45, and 60 min and quenched with 1 M urea. A thrombin digestion was performed to remove the MBP tag from the substrate/product(s) in the mix, and the McbA fragment was isolated by HPLC and subjected to ESI-mass spectrometry. For each oxazole or thiazole formed, a loss of 20 mass units is observed. The mass spectra collected (Figure 4A) show the early formation of product containing one ring (M-20) followed by formation of the two ring final product (M-40). Given the relative peak abundances of M, M-20, and M-40 peaks for each of the time points (t = 15, 30, 45, and 60 min), one can calculate the amount of heterocycles formed as 5.9, 13.9, 15.0, and 15.9 μM out of a total starting substrate concentration of 20 μM (20 μM × 2 = 40 μM ring-forming sites) (Table 3). The corresponding ADP formation trace is shown in Figure 4B and gives a linear rate of ATP hydrolysis of 1.74 μM/min. The ratio of ATP hydrolyzed to heterocycle formed is shown in the last column of Table 3. For the 15, 30, 45, and 60 min time points, the ratios of ATP hydrolyzed to the number of rings formed are 4.4, 3.7, 5.2, and 6.5, respectively. Errors in these values are determined by the accuracy of ESI/MS peak abundances and should be well below 20%. Thus, the stoichiometry of MccB17 synthetase ATP usage is 5 ± 1 ATP/heterocycle formed under these assay conditions.

Next, two MBP-McbA$_{1-46}$ substrate derivatives, MBP-McbA$_{1-46(GSG)}$ and MBP-McbA$_{1-46(GGC)}$, that differ greatly in their rate of modification by MccB17 synthetase (*20*) were examined as substrates in the TLC ATPase assay. These

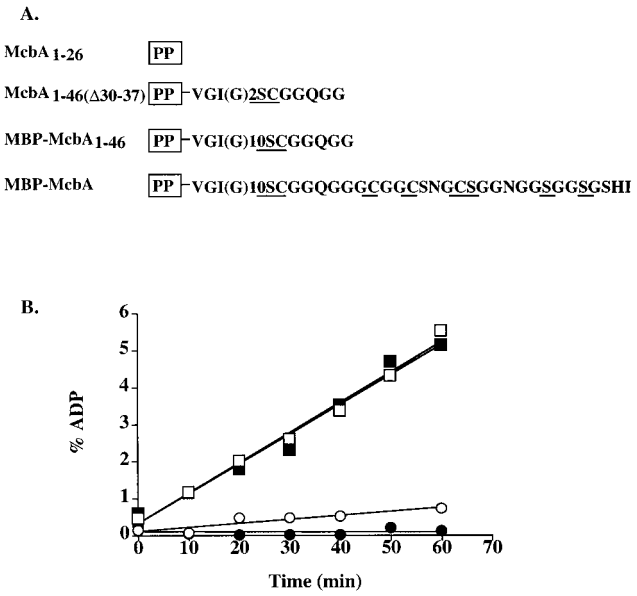

FIGURE 3: Substrate dependence of the ATPase/GTPase activity of MccB17 synthetase. (A) Fusion proteins and synthetic peptides used in a TLC assay to detect ATPase activity. $McbA_{1-26}-CONH_2$ is a synthetic version of the McbA propeptide, and $McbA_{1-46(\Delta30-37)}$ is a synthetic peptide derived from the first 46 amino acids of McbA sequence with 8 of the 10 internal Gly residues absent. MBP-$McbA_{1-46}$ is an MBP fusion protein encoding the first 46 residues of McbA, while MBP-McbA is an MBP fusion protein encoding full-length McbA (residues 1−69). MBP-$McbA_{1-46}$ contains the first two sites of modification, while MBP-McbA contains all eight sites. PP, propeptide sequence (residues 1−26 of McbA). (B) ATPase assay. Incubations with 0.05 mg/mL MccB17 synthetase, 1× MccB17 synthetase reaction buffer, [^{32}P]α-ATP, and either 20 μM $McbA_{1-26}-CONH_2$ (●), $McbA_{1-46(\Delta30-37)}$ (○), MBP-$McbA_{1-46}$ (■), or MBP-McbA (□), were performed at 37 °C. At the time points indicated, an aliquot of the reactions was removed and quenched with 0.5 M EDTA. The amount of ATP hydrolyzed was determined by TLC.

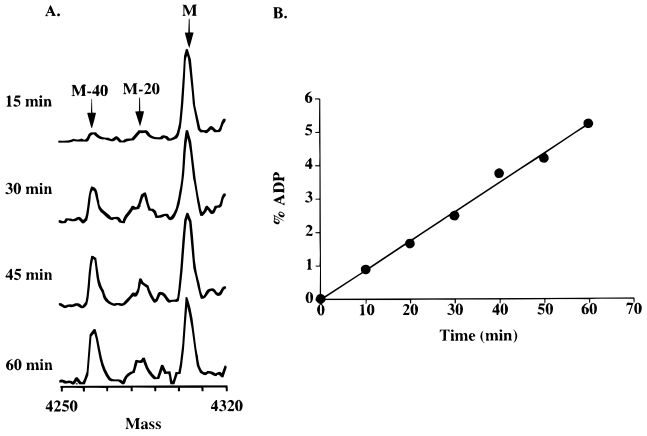

FIGURE 4: Stoichiometry of ATP hydrolysis and heterocycle formation. To determine the stoichiometry of ATP hydrolysis and heterocycle formation two reactions were run in parallel—one to follow heterocycle formation and one to follow ATP hydrolysis. (A) Mass spectrometry analysis of heterocycle formation. Incubations of 0.05 mg/mL MccB17 synthetase, 20 μM MBP-$McbA_{1-46}$, and 1× MccB17 synthetase reaction buffer were performed at 37 °C. Samples for mass spectrometry were prepared as described in the Experimental Procedures after 0, 15, 30, 45, and 60 min of incubation. M, unmodified substrate (4305 Da); M-20, mono-heterocyclic product (4285 Da); and M-40, bis-heterocyclic product (4265 Da). (B) ATPase activity. Incubations were performed as described in (A) except that [^{32}P]α-ATP was included in the reaction mix. At the times indicated, an aliquot was removed and quenched with 0.5 M EDTA. The amount of ATP hydrolyzed was determined by TLC.

Table 3: Stoichiometry of ATP Hydrolysis and Heterocycle Formation

time (min)	ATP hydrolyzed[a] (μM)	heterocycles[b] (μM)	ATP:Heterocycles[c]
15	26.1	5.9	4.4
30	52.2	13.9	3.7
45	78.3	15.0	5.2
60	104.4	15.9	6.5

[a] The amount of ATP hydrolyzed at each time point was determined by TLC as described in the Experimental Procedures. [b] The amount of heterocycles formed at each time point was determined by ESI-MS by calculating the peak abundances of the M, M-20, and M-40 as described in the Experimental Procedures. [c] The stoichiometry of ATP hydrolysis to heterocycle formation was calculated according to the following equation for each time point: [ATP]/[Heterocycle].

two substrates are variations of MBP-$McbA_{1-46}$, that each contain only one potential site for heterocyclic modification. In MBP-$McbA_{1-46(GSG)}$, Cys_{41} is replaced by Gly, and in MBP-$McbA_{1-46(GGC)}$, Ser_{40} is replaced by Gly (*20*). Although MBP-$McbA_{1-46(GGC)}$ is processed to heterocyclic thiazole at an initial rate that is essentially equivalent to the MBP-$McbA_{1-46}$ substrate (Figure 5A), it induces a 7-fold lower ATPase activity than the MBP-$McbA_{1-46}$ substrate (Figure 5B). The similar rates of heterocycle formation reflect similar rates of first ring formation. However, in the ATPase assay that is measured over a 60 min time course, two-ring product (M-40) is observed with the MBP-$McbA_{1-46}$ as substrate and so the higher rate of ATPase activity with this substrate may reflect the ATP hydrolysis required to go on to the bis-heterocyclic product. Likewise, the MBP-$McbA_{1-46(GSG)}$ substrate which is modified at a low, but detectable rate (7-fold lower than MBP-$McbA_{1-46}$) to monooxazole product, induces a slow rate of ATP hydrolysis (at least 20-fold lower than the MBP-$McbA_{1-46}$) (Figure 5).

In an effort to improve signal-to-noise, we several times attempted to conduct incubations of MBP-$McbA_{1-46}$ at concentrations higher than 20 μM ($10K_m$). For example, when incubations were carried out at 100 μM substrate to accumulate more product for mass spectrometry analysis, the studies were thwarted by substantial substrate inhibition. The inhibition is most readily assessed in Western blot assays (Figure 6A) with heterocyclic product formation decreasing linearly between 50 and 200 μM substrate. The basis for this inhibition is presently unknown, but is not due to lack of solubility of the fusion protein (but could be due to concentration-dependent oligomerization) and is not an artifact of the Western assay as UV−vis spectroscopy (single heterocycles give an absorbance at 254 nm, while 4,2 bis-heterocycles give an absorbance at 280 nm) (*20*) and mass spectrometry analysis (data not shown) also confirmed the suppression of heterocyclization. However, under these conditions, the substrate-dependent ATPase activity of MccB17 synthetase was not shut down nor noticeably inhibited as shown in Figure 6B. Under these conditions, the induced ATPase activity is clearly uncoupled from the ring formation process.

McbD as a Candidate for the Conditional ATPase/GTPase Activity of Microcin B17 Synthetase. Given the detection of a heterocyclizable substrate-regulated ATPase/GTPase

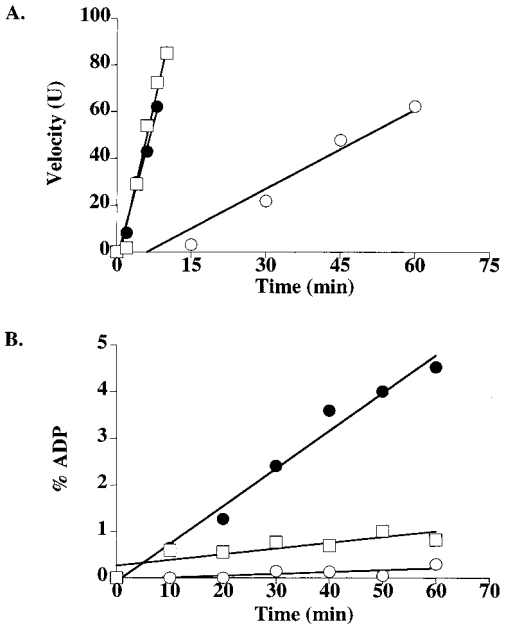

FIGURE 5: Comparison of MBP-McbA$_{1-46}$, MBP-McbA$_{1-46(GSG)}$, or MBP-McbA$_{1-46(GGC)}$ as substrates in the Western blot and ATPase assays. (A) Western blot assay. Incubations of 0.05 mg/mL MccB17 synthetase, 1× MccB17 synthetase reaction buffer, and either 20 μM MBP-McbA$_{1-46}$ (●), MBP-McbA$_{1-46(GSG)}$ (○), or MBP-McbA$_{1-46(GGC)}$ (□) were performed at 37 °C. At t = 0, 2, 4, 6, 8, and 10 min (MBP-McbA$_{1-46}$ and McbA$_{1-46(GGC)}$) or at t = 0, 15, 30, 45, and 60 min [MBP-McbA$_{1-46(GSG)}$], an aliquot of the reactions was removed and quenched with SDS−PAGE sample buffer. Samples were analyzed by SDS−PAGE followed by Western blotting as described in the Experimental Procedures. (B) ATPase assay. Incubations of 0.05 mg/mL MccB17 synthetase, 1× MccB17 synthetase reaction buffer, [^{32}P]α-ATP, and either MBP-McbA$_{1-46}$ (●), MBP-McbA$_{1-46(GSG)}$ (○), or MBP-McbA$_{1-46(GGC)}$ (□) were performed at 37 °C. At the time points indicated, an aliquot of the reactions was removed and quenched with 0.5 M EDTA. The amount of ATP hydrolyzed was determined by TLC.

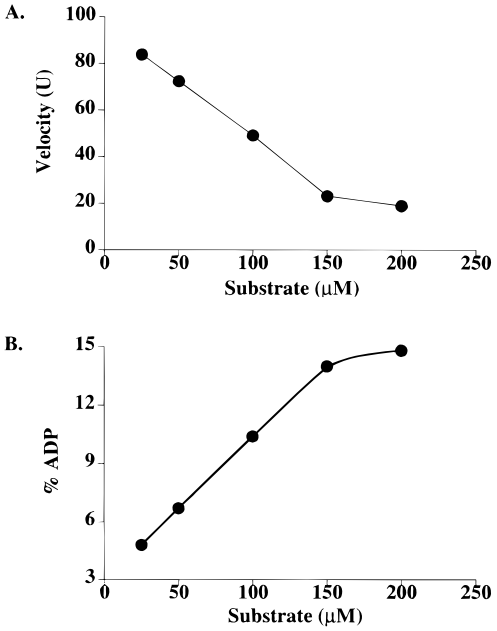

FIGURE 6: Heterocycle formation and ATP hydrolysis at high substrate concentrations. (A) Heterocycle formation. Product formation was assessed by Western blotting. Incubations of 0.05 mg/mL MccB17 synthetase, 1× MccB17 synthetase reaction buffer, and either 0, 25, 50, 100, 150, or 200 μM MBP-McbA$_{1-46}$ were performed at 37 °C. At t = 5 min, an aliquot of the reactions was removed and quenched with SDS−PAGE sample buffer. Samples were analyzed by SDS−PAGE followed by Western blotting as described in the Experimental Procedures. (B) ATPase assay. Incubations of 0.05 mg/mL MccB17 synthetase, 1× MccB17 synthetase reaction buffer, [^{32}P]α-ATP, and either 25, 50, 100, 150, or 200 μM MBP-McbA$_{1-46}$ were performed at 37 °C. At t = 0, 10, 20, 30, 40, 50, and 60 min, an aliquot of the reactions was removed and quenched with 0.5 M EDTA. Samples were then analyzed by TLC. The ATPase activity observed for the McbB17 synthetase alone and for substrate alone (25−200 μM) was subtracted from the data obtained for MccB17 synthetase plus substrate.

```
  1 MINVYSNLMS AWPATMAMSP KLNRNMPTFS QIWDYERITP ASAAGETLKS
                                                  *  *
                                                  A
 51 IQGAIGEYFE RRHFFNEIVT GGQKTLYEMM PPSAAKAFTE AFFQISSLTR
                                  *
101 DEIITHKFKT VRAFNLFSLE QQEIPAVIIA LDNITAADDL KFYPDRDTCG
                                  B                  *  *
151 CSFHGSLNDA IEGSLCEFME RQSLLLYWLQ GKANTEISSE IVTGINHIDE
                                                  *  *
201 ILLALRSEGD IRIFDITLPG APGHAVLTLY GTKNKISRIK YSTGLSYANS
251 LKKALCKSVV ELWQSYICLH NFLIGGYTDD DIIDSYQRHF MSCNKYESFT
301 DLCENTVLLS DDVKLTLEEN ITSDTNLLNY LQQISDNIFV YYARERVSNS
351 LVWYTKIVSP DFFLHMNNSG AININNKIYH TGDGIKVRES KMVPFP
```

FIGURE 7: Amino acid sequence of McbD. The sequence is presented as previously published with the exception of a change at position 171 (a Thr to Arg change; codon change ACA to AGA at codon 171; bases 511−513). This discrepancy was discovered during sequencing of the wild-type MccB17 plasmid, pPY113 (*13*). The putative Walker A and Walker B sequences are underlined and labeled, A and B, respectively. The consensus motifs that define the nucleotide-binding site in conditional GTPases are underlined and in bold. Residues mutated individually to Ala are indicated by an asterisk.

activity in the three subunit synthetase (McbB, C, D), we examined the protein sequence of each subunit for possible motifs for purine triphosphate recognition. Initial searches with the sequences of McbB, C, and D did not reveal significant homology or a known motif. In particular, the telltale signature of the Walker A box (phosphate binding loop) GXGXXGK(S/T) (*25*, *26*) was not detectable in any of the three proteins. On closer analysis though, the sequence of the 45 kDa McbD (Figure 7) provided some intriguing hints. For many ATP and GTP hydrolyzing enzymes there is also a Walker B box (*25*) of four hydrophobic residues followed by Asp (or Glu) which is a ligand to Mg^{2+} in the active site. McbD has IIALD at residues 128−132. A sequence potentially reminiscent of a Walker A motif, AAGETLKS, is located at residues 43−50. More intriguingly, two of the three consensus motifs that define the nucleotide-binding site G1, G2, and G3 of conditional GTPases (*27*) are present in McbD as shown in Table 4: namely the DXXG motif (DTCG, 147−150) which is involved in conformational switching between the GDP and GTP forms and the NXXD motif (NHID, 196−199) that provides specificity for guanine in G proteins and were thus good candidates for mutagenesis.

Although we can overproduce the McbD subunit on its own and purify it as a fusion to MBP, MBP-McbD, we do not have an assay for its activity. It does not show unregulated ATPase/GTPase activity alone nor does addition of substrate, MBP-McbA$_{1-46}$, induce ATPase activity (data not shown). To address the possibility that McbD was the ATPase, we made mutations in McbD at some of the above sites proposed to be important for NTPase activity in the context of the entire MccB17 biosynthetic operon present on plasmid pUC19mccb17. This plasmid directs the expression of both MccB17 synthetase and pre-MccB17, and thus,

Table 4: GTP Consensus Motifs

protein	no. of amino acid residues	I,[a] GXXXXGKS/T	II,[b] $\phi\phi\phi\phi\phi$D	III,[c] DXXG	IV,[d] NXXD
McbD	396	AAGETLKS	VIIALD	DTCG	NHID
		43 50	127 132	147 150	196 199
Ras-p21	166	GAGGVGKS	GFLCVF	DTAG	NKCD
		10 17	77 82	57 60	116 119
ARF-1	180	GLDAAGKT		DVGG	NKQD
		23 30		66 69	125 128
Ran	216	GDGGTGKT		DTAG	NKVD
		17 24		65 68	122 125
Gtα	324	GAGESGKS	CIIFIA	DVGG	NKKD
		11 18	190 195	70 73	239 242
Giα	353	GAGESGKS	AIIFCV	DVGG	NKKD
		39 46	219 224	199 202	268 271
EF-Tu	394	GHVDHGKT	GAILVV	DCPG	NKCD
		19 26	101 106	81 84	136 139

[a] Walker A. [b] Walker B. [c] Conformational change, D binds Mg^{2+}. [d] Guanine recognition motif.

strains of *E. coli* carrying this plasmid produce mature MccB17 antibiotic. The effect of the McbD mutations can be assessed both by quantitating antibiotic production in a bioassay and by measuring MccB17 synthetase activity in crude cell extracts. The residues, G45, K49, D132, D147, G150, N196, and D199 were individually replaced by Ala by PCR mutagenesis. G45 was targeted as a potential equivalent of the Ras Gly-12 residue which is involved in oncogenic activation (*28*). K49 was a candidate for the conserved Lys residue involved in phosphate binding present in the Walker A motif of many ATPases and GTPases (*25*). D132 is present in the putative Walker B motif in which it would be involved in Mg^{2+} binding at the active site (*25*). D147 and G150 are predicted to be involved in conformational switching, while N196 and D199 would define the NTP specificity in G protein families (*27*). The wild-type and mutant pUC19mccb17/DH5α strains were used to assess how the McbD mutations affected antibiotic activity and enzymatic activity of MccB17 synthetase.

Production of the active antibiotic MccB17 by the mutant strains was assessed in a liquid culture bioassay. Briefly, MccB17-containing extracts from the wild-type and mutant strains were prepared as described in the Experimental Procedures and added to a culture of a MccB17-sensitive strain, ZK4. After 5 h of growth in the presence of the extract, the OD_{600} was determined. In this assay, extract containing mature MccB17 antibiotic causes a decrease in the OD_{600} due to cell killing. The D132A and D147A mutants are severely compromised and D199A retains only partial activity (approximately 3-fold down from wild-type) consistent with some defect in antibiotic synthesis or maturation (Figure 8A). The G45A, K49A, G150A, and N196A mutants exhibited the same or greater antibiotic activity as the wild-type strain (Figure 8A).

These studies were followed up by examining MccB17 synthetase activity in crude cell extracts prepared from the wild-type and mutant pUC19mccb17/DH5α strains. The data of Figure 8B show the activity of the mutant MccB17 synthetases as compared to wild-type synthetase in the Western assay monitoring heterocycle formation. Consistent with the bioassay results, the D132A and D147A are the most severely affected, and D199A retains partial activity. Interestingly, although antibiotic production by the G45A mutant appeared essentially unaffected in the bioassay, this mutant synthetase in crude extract is clearly less active than

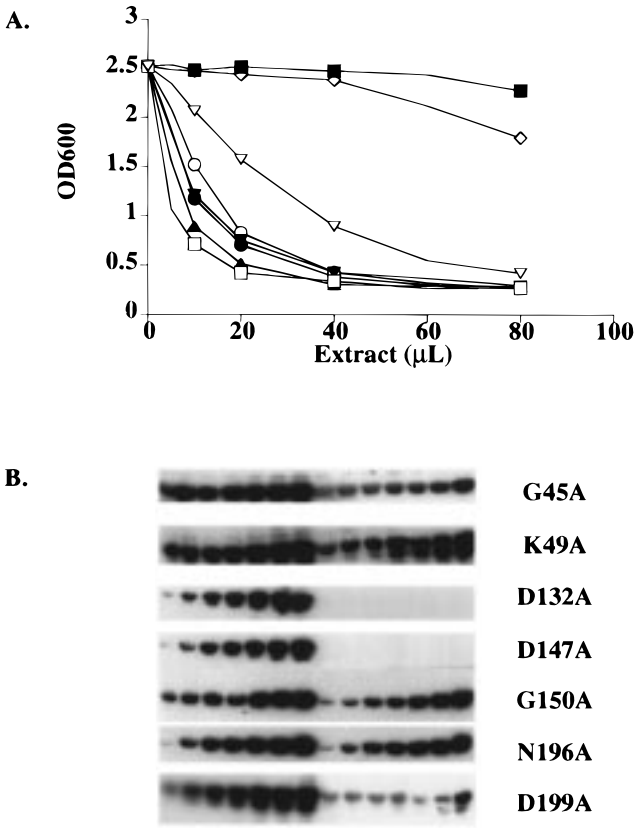

FIGURE 8: Analysis of McbD mutants. (A) Antibiotic production by McbD mutant MccB17 sythetases. MccB17 synthetase mutants, G45A (○), K49A (▲), D132A (◇), D147A (■), G150A (▼), N196A (□), and D199A (▽) were analyzed for their ability to produce active MccB17 antibiotic in a liquid culture bioassay as described in the Experimental Procedures. (B) Heterocycle forming activity of McbD mutant MccB17 synthetases. MccB17 synthetase mutants, G45A, K49A, D132A, D147A, G150A, N196A, and D199A were analyzed for their ability to form heterocycles in vitro. Crude extracts from pUC19mccb17 mutant and wild-type strains were incubated with 20 μM MBP-McbA$_{1-46}$ and 1× MccB17 synthetase reaction buffer. At 5, 10, 15, 20, 30, 45, and 90 min, an aliquot of the reactions was removed and quenched with SDS-sample buffer. Samples were then analyzed by SDS−PAGE followed by Western blotting as described in the Experimental Procedures. The first seven lanes of each blot correspond to wild-yype synthetase, while the last seven lanes correspond to the mutant synthetase.

wild-type synthetase. The K49A mutant appears to exhibit wild-type levels of synthetase activity and, thus, is not a candidate for an essential Lys residue in a putative phosphate-

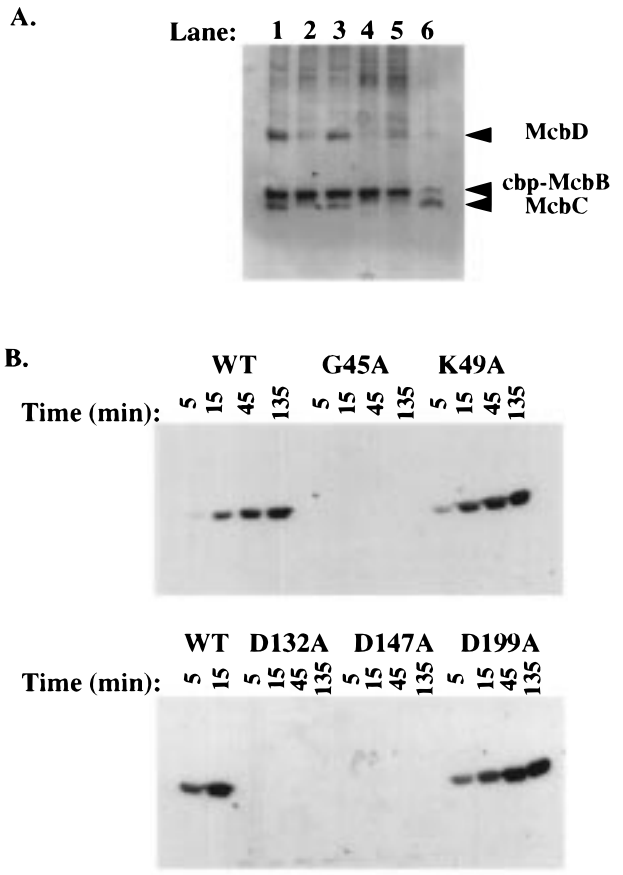

FIGURE 9: Purification and analysis of mutant CBP-tagged MccB17 synthetases. CBP-tagged versions of MccB17 sythetase carrying mutations in the McbD subunit and the wild-type version (WT, lane 1; G45A, lane 2; K49A, lane 3; D132A, lane 4; D147A, lane 5; or D199A, lane 6) were purified by the standard protocol using calmodulin affinity chromatography. (A) SDS−PAGE analysis of the purified mutant CBP-tagged MccB17 synthetase complexes. (B) Western blot assay of reactions using the mutant CBP-tagged MccB17 synthetases. Incubations were performed using 0.05 mg/mL mutant or wild-type synthetase, 20 μM MBP-McbA$_{1-46}$ as substrate, and 1× MccB17 synthetase reaction buffer. At the times indicated, an aliquot of the reactions was removed and quenched with SDS-sample buffer. The samples were analyzed by SDS−PAGE followed by Western blotting as described in the Experimental Procedures.

binding loop. The mutations G150A and N196A also appear to have no affect on MccB17 synthetase activity.

In an effort to assess the effect of these mutations on the ATPase activity of purified MccB17 synthetase, the G45A, K49A, D132A, D147A, and D199A mutations were created in the MccB17 synthetase expression construct, pCALBCDn. These mutant synthetases were expressed and purified by calmodulin affinity chromatography. Three of the mutant synthetases, G45A, D132A, and D147A, did not purify like wild-type synthetase (upon repeated attempts) in that the McbD and McbC subunits in the fractions eluted from the calmodulin column were in low abundance (compared to wild-type CBP-tagged MccB17 synthetase) or completely absent suggesting that these mutations affected complex assembly or stability (Figure 9A). A synthetase assay was performed using the CBP-tagged material purified for each mutant and wild-type synthetase. The three mutant synthetases that did not purify like wild-type enzyme did not exhibit any detectable activity, while the K49A mutant had wild-type activity and the D199A was approximately 3-fold down in activity as compared to wild-type synthetase (Figure 9B).

Taken together, the results of the mutational analysis indicate that mutations in some residues that are conserved and involved in GTP binding in the broad category of small G proteins are deleterious to MccB17 synthetase heterocyclization activity, while others (K49, N196) are not essential, indicating a distinct pattern of nucleoside triphosphate binding for McbD.

DISCUSSION

These studies establish that the multimeric enzyme complex MccB17 synthetase that cyclizes four Ser and four Cys residues to oxazoles and thiazoles in McbA shows an absolute requirement for ATP or GTP cleavage. In the absence of ATP or GTP, no peptide heterocyclic products were detectable by polyclonal antibody, which detects as few as one of the thiazole or oxazole rings. The 80-fold reduction in rate of heterocyclic peptide production in the presence of ATP-γ-S, chemically sluggish toward thiophosphoryl transfer because of the sulfur substitution, suggests that the phosphoryl-transfer step with that ATP analogue is substantially rate determining for thiazole and oxazole formation.

The MccB17 synthetase complex, purified either as wild-type three subunit enzyme (*14*) or with a calmodulin binding peptide tag at the N-terminus of McbB to allow affinity isolation (*16*), has negligible ATPase activity in the absence of substrate and so qualifies as a conditional or substrate-dependent ATPase/GTPase. We note in passing that our original isolation (*14*) of the synthetase resulted in copurification of the chaperone HtpG (*29*, *30*), which could have slow ATPase activity (*31*, *32*). We have since purified the synthetase from an *E. coli* strain (MC4100 Δ*htpG* pPY113) deleted for *htp*G and the synthetase is still active and ATP-requiring (J.C.M., B. Nickels, and C.T.W., unpublished experiments). Also, the affinity-purified enzyme used in most of these studies is similarly free of any detectable HtpG (*16*).

Addition of McbA substrates elicits the ATPase activity along with heterocycle formation. ATP/GTP hydrolysis and peptide substrate turnover is in general coupled. Thus, the McbA$_{1-26}$ propeptide which binds with low micromolar affinity does not induce ATPase activity nor does a McbA peptide with Gly 30−37 deleted [McbA$_{1-46(\Delta 30-37)}$]. The single-site substrate MBP-McbA$_{1-46(GGC)}$ does induce turnover-dependent ADP formation but at a slower initial velocity than the two-site substrate, MBP-McbA$_{1-46}$. However, by Western blot analysis measuring thiazole and oxazole formation, these two substrates exhibit the same initial rate of modification. The MBP-McbA$_{1-46(GSG)}$ substrate is only very slowly processed and shows a very slow rate of ADP production. These observations suggest a coupling of purine triphosphate hydrolysis to heterocycle formation, but suggest that differential efficiency is possible.

To determine the stoichiometry of ATP hydrolysis to heterocycle formation, we have employed electrospray ionization to generate multiply charged substrate (M), one ring product (M-20), and two ring product (M-40) using the MBP-McbA$_{1-46}$ protein as substrate. Although no calibration standards exist for the M-20 and M-40 enzymatic products, major differences in ionization efficiency (i.e., >10%) have been ruled out by careful correlation of UV absorbance and

ESI/MS peak intensities (*20*). The time course data presented in Table 3 show an average ratio of ATP/heterocycle (thiazole or oxazole) of 5 ± 1.

When the MBP-McbA$_{1-46}$ substrate concentration is raised from 10K_m to greater than 50K_m values (20 to > 100 μM), there is profound inhibition of heterocycle formation. Perhaps a second site is being occupied on the synthetase, perhaps the fusion protein is oligomerizing, or perhaps some other even less well-defined phenomenon is occurring. In any event, the ATPase activity is not comparably inhibited and thus becomes almost completely uncoupled under these conditions. This uncoupled ATPase activity requires substrate given all the above observations showing no ATPase activity when substrate is absent.

With these observations, the question arises as to the thermodynamic and mechanistic roles of ATP in MccB17 synthetase-mediated Ser and Cys residue heterocyclization. That ATP/GTP hydrolysis is tightly regulated (i.e., only turned on in the presence of a modifiable substrate) is as expected to avoid wasteful expenditure of cellular energy. We have considered two general mechanistic alternatives for coupled ATPase and thiazole/oxazole ring formation: (1) transfer of the $-PO_3$ group of ATP to some peptide intermediate to chemically facilitate one or more aspects of the cyclization/dehydration/dehydrogenation process; (2) a coupled conformational switch between enzyme ATP/GTP and enzyme ADP/GDP forms that may bind substrate differentially or have some motor or chaperone function. While phosphorylation of the oxyanion originating from the amide carbonyl upon cyclization (via attack of Ser or Cys side chains) would be a route to lower the energy barrier to cyclodehydration (thiazoline and oxazoline formation), the stoichiometry data of greater than 1 ATP hydrolyzed for each heterocycle formed support the second mechanistic alternative unless nonproductive $-PO_3$ transfer can occur (e.g., dissipation of four out of five reaction intermediates via hydrolysis without heterocyclization).

The second mechanistic alternative for coupled ATP/GTP hydrolysis would not involve the chemical transfer of the $-PO_3$ group to peptide heterocyclization intermediates. Instead, the molecular logic of ATP-dependent chaperones (*33, 34*), ATP and GTP-dependent motor proteins (*35*), or GTP-cleaving G proteins may be relevant (*27, 36*). In all three protein families, purine triphosphate cleavage drives a conversion to a distinct conformational state of the ATPase/GTPase domain that results in differential interactions with effector proteins and/or substrates in the ADP/GDP versus ATP/GTP-bound states. In the case of motor proteins, ATP/GTP hydrolysis effects a coupled step movement along substrate (*35*). For many G proteins (EF-Tu, SRP, Rabs), transport or movement of associated partner proteins is the net outcome of coupled GTP hydrolysis (*37*−*39*). As with these examples, the ATP/GTP conformation of MccB17 synthetase may be distinct from that of the ADP/GDP conformation and thus may regulate or direct protein recognition and/or interactions.

For MccB17 synthetase, the high-affinity binding site on substrate McbA is not at any of the eight cyclization sites between residues 39 and 69 but rather at the helical propeptide at residues 1−26 (*14, 17, 18*). We have shown previously that the propeptide must be covalently connected in cis to direct heterocyclization (*14*). Thus, there is a formal requirement for the three subunit synthetase to dock at propeptide and then simultaneously or sequentially at the eight downstream cyclization sites in McbA. Nucleotide hydrolysis cannot be linked to formation of an enzyme−substrate complex, because a synthetic propeptide, McbA$_{1-26}$, binds tightly to synthetase (with a K_i value equivalent to the K_m for McbA substrate) but does not induce ATP hydrolysis. Instead, MccB17 synthetase may dock at the propeptide, and couple the hydrolysis of ATP/GTP to movement along the McbA substrate. Alternatively, the synthetase may dock at the propeptide and couple hydrolysis to bringing the target sequences to the active site of the synthetase. This mechanism may explain the absolute requirement for the propeptide to be in cis rather than trans. Yet another possibility is that nucleotide hydrolysis is required in the release of the product heterocycle from the active site so that the next substrate site can be modified. While we have data that MccB17 synthetase can act distributively rather than processively (N.L.K., and C.T.W., unpublished experiments), we do not have evidence yet of directional processing (e.g., N → C heterocyclization) and so no evidence yet for a motor function for the coupled ATPase/GTPase.

The function of each of the required three subunits McbB, McbC, and McbD in the MccB17 synthetase complex is currently being investigated. McbB contains stoichiometric amounts of zinc (J.C.M., A. Woklu, C.T.W., unpublished results) and may be the cyclization/dehydration catalyst. McbC contains 1 equiv of FMN (*14*) and is a candidate for the last step in heterocycle production, the introduction of the C═C double bond as the thiazoline and oxazoline intermediates are desaturated to thiazole and oxazole. It is unlikely that McbB or C have any role in GTP or ATP hydrolysis. On the other hand, the role of McbD could be the conditional ATPase/GTPase. The first 200 amino acids of the 396 amino acid McbD subunit bear some, but not all, of the consensus sequence hallmarks of ATP and GTP recognizing enzymes. The most characteristic of these motifs, the Walker A sequence [GXGXXGK(S/T)], that is the glycine-rich P loop that binds the α and β phosphates of GTP/ATP and GDP/ADP (*25*), is not present in a recognizable form. However, there are many ATP-cleaving enzymes, e.g., the ATP grasp fold family where the P loop is not detectable by sequence inspection (*40*). A good candidate for the second Walker sequence, the B box, defined as four hydrophobics followed by Asp (or Glu) (*25*), is present in McbD at residues 128−132. The Asp/Glu (D132 in McbD) is thought to participate in Mg^{2+} coordination at the active site and/or activation of the water molecule that attacks the $-PO_3$ group in the catalytic step of hydrolysis of such GTPases/ATPases.

Particularly intriguing is the presence, in the canonical order, of two of the GTP-binding motifs that define the common structural core for GDP or GTP binding in the G protein superfamily (*27, 36*) as noted in Table 4. The DXXG loop (residues 147−150 in McbD) in G proteins whose structures are known is often close to the P loop. The invariant Asp (D147 in McbD) binds the catalytic Mg^{2+} through a coordinated water molecule, while the amide proton of the invariant Gly forms a hydrogen bond with the γ-phosphate of GTP (*27, 36*). The NXXD consensus (residues 196−199 in McbD) is typically a stretch that interacts with the purine ring and helps specify guanine recognition (*27, 36*). The carboxy oxygens of Asp (D199 in McbD) form hydrogen bonds with groups on the guanine

ring, while amide protons of the Asn stabilize the nucleotide-binding site through hydrogen bonds with residues present in the Walker A sequence (*27*, *36*).

A first test of the proposition that McbD may be the conditional ATPase/GTPase of the MccB17 synthetase complex involved the construction of the seven mutants shown in Figure 7. As we have no direct assay for the isolated McbD subunit, these mutants were evaluated for their effects on MccB17 antibiotic production and MccB17 synthetase heterocyclization activity. Most notable is the curtailment of activity in the three Asp to Ala mutants, D132A, D147A, and D199A, given the function of those Asp residues in well-characterized conditional GTPases. The inability to purify several of the mutant synthetase complexes (G45A, D132A, and D147A) further suggests that this region of McbD may be important in subunit interactions or complex stability.

These data support the hypothesis that McbD is the protein−substrate-regulated ATPase/GTPase, but more direct evidence will be required to definitively prove that McbD binds and hydrolyzes ATP/GTP, given that K49A and N196A mutations had no effect. The relatively high K_m for ATP and GTP, the likely rapid release of ADP and GDP, and the equivalent catalytic efficiency of each purine nucleoside triphosphate will make McbD functionally and probably architecturally distinct from canonical tight binding G protein conditional GTPases, such as the *E. coli* EF-Tu (*37*). In its ability to use ATP, GTP, and even ITP, the *E. coli* McbD may bear analogy in its nucleotide binding site to another *E. coli* enzyme, succinyl CoA synthetase (*41*).

Further analysis of the role of ATP and GTP hydrolysis and validation that McbD is the subunit with turnover-dependent ATPase/GTPase activity will enhance our understanding of how the five-membered thiazole and oxazole rings are constructed in this DNA gyrase-targeted antibiotic. Such studies will also serve as a baseline to dissect the enzymatic logic for construction of other bioactive peptide heterocyclic natural products.

ACKNOWLEDGMENT

We are grateful to Dr. Ranabir Sinha Roy, Dr. Peter J. Belshaw, Dr. Jun Wang, and Dr. Yueming Li for helpful discussions. We thank Dr. Yueming Li for assistance in the design and construction of the pUC19mccb17 construct. Mass spectral data were obtained at the Boston University School of Medicine Mass Spectrometry Resource, which is supported by NIH/NCRR (Grant P41-RR10888 and Grant S10-RR10493 to Dr. C. E. Costello).

REFERENCES

1. Sahl, H. G., Jack, R. W., and Bierbaum, G. (1995) *Eur. J. Biochem. 230*, 827−853.
2. Roach, P. L., Clifton, I. J., Hensgens, C. M. H., Shibata, N., Schofield, C. J., Hajdu, J., and Baldwin, J. E. (1997) *Nature 387*, 827−830.
3. Stubbe, J., Kozarich, J. W., Wu, W., and Vanderwall, D. E. (1996) *Acc. Chem. Res. 29*, 322−330.
4. Floss, H. G. and Beale, J. M. (1989) *Angew. Chem., Int. Ed. Engl. 28*, 146−177.
5. Selva, E., Beretta, G., Monianini, N., Saddler, G. S., Gastaldo, L., Ferrari, P., Lorenzetti, R., Landini, P., Ripamonti, F., Goldstein, B. P., Berti, M., Montanaro, L., and Denaro, M. (1991) *J. Antibiot. 44*, 693−701.
6. Elbein, A. D. (1984) *CRC Crit. Rev. Biochem. 16*, 21−49.
7. Bayer, A., Freund, S., Nicholson, G., and Jung, G. (1993) *Angew. Chem., Int. Ed. Engl. 32*, 1336−1339.
8. Yorgey, P., Lee, J., Kordel, J., Vivas, E., Warner, P., Jebaratnam, D., and Kolter, R. (1994) *Proc. Natl. Acad. Sci. U.S.A. 91*, 4519−4523.
9. Bayer, A., Freund, S., and Jung, G. (1995) *Eur. J. Biochem. 234*, 414−426.
10. San Millan, J. L., Kolter, R., and Moreno, F. (1985) *J. Bacteriol. 163*, 1016−1020.
11. San Millan, J. L., Hernandez-Chico, C., Pereda, P., and Moreno, F. (1985) *J. Bacteriol. 163*, 275−281.
12. Vizan, J. L., Hernandez-Chico, C., del Castillo, I., and Moreno, F. (1991) *EMBO J. 10*, 467−476.
13. Yorgey, P., Davagnino, J., and Kolter, R. (1993) *Mol. Microbiol. 9*, 897−905.
14. Li, Y. M., Milne, J. C., Madison, L. L., Kolter, R., and Walsh, C. T. (1996) *Science 274*, 1188−1193.
15. Garrido, M. C., Herrero, M., Kolter, R., and Moreno, F. (1988) *EMBO J. 7*, 1853−1862.
16. Sinha Roy, R., Belshaw, P. J., and Walsh, C. T. (1998) *Biochemistry 37*, 4125−4136.
17. Madison, L. L., Vivas, E. I., Li, Y. M., Walsh, C. T., and Kolter, R. (1997) *Mol. Microbiol. 23*, 161−168.
18. Sinha Roy, R., Kim, S., Baleja, J. D., and Walsh, C. T. (1998) *Chem. Biol. 5*, 217−228.
19. Fields, G. B. a. N., R. L. (1990) *Int. J. Pept. Protein Res. 35*, 161−214.
20. Belshaw, P. J., Sinha Roy, R., Kelleher, N. L., and Walsh, C. T. (1998) *Chem. Biol. 5*, 373−384.
21. Sambrook, J., Fritsch, E. F., and Maniatis, T. (1989) *Molecular Cloning: A Laboratory Manual*, 2nd ed., Cold Spring Harbor Laboratory, Plainview, NY.
22. McCafferty, D. G., Lessard, I. A. D., and Walsh, C. T. (1997) *Biochemistry 36*, 10498−10505.
23. Pace, C. N., Vajdos, F., Fee, L., Grimsley, G., and Gray, T. (1995) *Protein Sci. 4*, 2411−2423.
24. Fenn, J. B., Mann, M., Meng, C. K., Wong, S. F., and Whitehouse, C. M. (1990) *Mass Spectrom. Rev. 9*, 37−70.
25. Walker, J. E., Saraste, M., Runswick, M. J., and Gay, N. J. (1982) *EMBO J. 1*, 945−951.
26. Saraste, M., Sibbald, P. R., and Wittinghofer, A. (1990) *Trends Biochem. Sci. 15*, 430−434.
27. Kjeldgaard, M., Nyborg, J., and Clark, B. F. (1996) *FASEB J. 10*, 1347−1368.
28. Seeburg, P. H., Colby, W. W., Capon, D. J., Goeddel, D. V., and Levinson, A. D. (1984) *Nature 312*, 71−75.
29. Bardwell, J. C. A. a. C., E. A. (1987) *Proc. Natl. Acad. Sci. U.S.A. 84*, 5177−5181.
30. Bardwell, J. C. A. a. C., E. A. (1988) *J. Bacteriol. 170*, 2977−2983.
31. Nadeau, K., Sullivan, M. A., Bradley, M., Engman, D. M., and Walsh, C. T. (1993) *J. Biol. Chem. 268*, 1479−1487.
32. Prodromou, C., Roe, S. M., O'Brien, R., Ladbury, J. E., Piper, P. W., and Pearl, L. H. (1997) *Cell 90*, 65−75.
33. Flynn, G. C., Chapell, T. G., and Rothman, J. E. (1991) *Science 245*, 385−390.
34. Roseman, A. M., Chen, S., White, H., Braig, K., and Saibil, H. R. (1996) *Cell 87*, 241−251.
35. Trayer, I. P. a. S., K. J. (1997) *Trends Cell Biol. 7*, 259−263.
36. Bourne, H. R., Sanders, D. A., and McCormick, F. (1991) *Nature 349*, 117−127.
37. Berchtold, H., Reshetnikova, L., Reiser, C. O. A., Schirmer, N. K., Sprinzi, M., and Hilgenfeld, R. (1993) *Nature 365*, 126−132.
38. Freymann, D. M., Keenan, R. J., Stroud, R. M., and Walter, P. (1997) *Nature 385*, 361−364.
39. Rybin, V., Ullrich, O., Rubino, M., Alexandrov, K., Simon, I., Seabra, M. C., Goody, R., and Zerial, M. (1996) *Nature 383*, 266−269.
40. Galperin, M. Y. a. K., E. V. (1997) *Protein Sci. 6*, 2639−2643.
41. Wolodko, W. T., Fraser, M. E., James, M. N. G., and Bridger, W. A. (1994) *J. Biol. Chem. 269*, 10883−10890.

BI980996E